Electronic Supplementary Material (ESI) for Journal of Materials Chemistry A.

A Dual-Functional Interlayer for Li-S Batteries by using Carbon Fiber Film Cladded Electronic-Deficiency $Li_2B_4O_7$

Xin Dai,[a] Kunyang Zou,[a] Weitao Jing,[a] Peng Xu,[b] Junjie Sun,[a] Shengwu Guo,[a] Qiang Tan,[a] Yongning Liu,[a] Tengfei Zhou[c]* and Yuanzhen Chen[a]*

a. State Key Laboratory for Mechanical Behavior of Materials, School of Materials Science and Engineering, Xi'an Jiaotong University, Xi'an 710049, P.R. China

b. Technical Monitoring Center, Petro China Changqing Oil Field Company, Xi'an, 710018, P.R. China

c. Institutes of Physical Science and Information Technology, Anhui University, Hefei, 230601, P.R. China

*Corresponding author: tengfeiz@ahu.edu.cn; cyz1984@xjtu.edu.cn

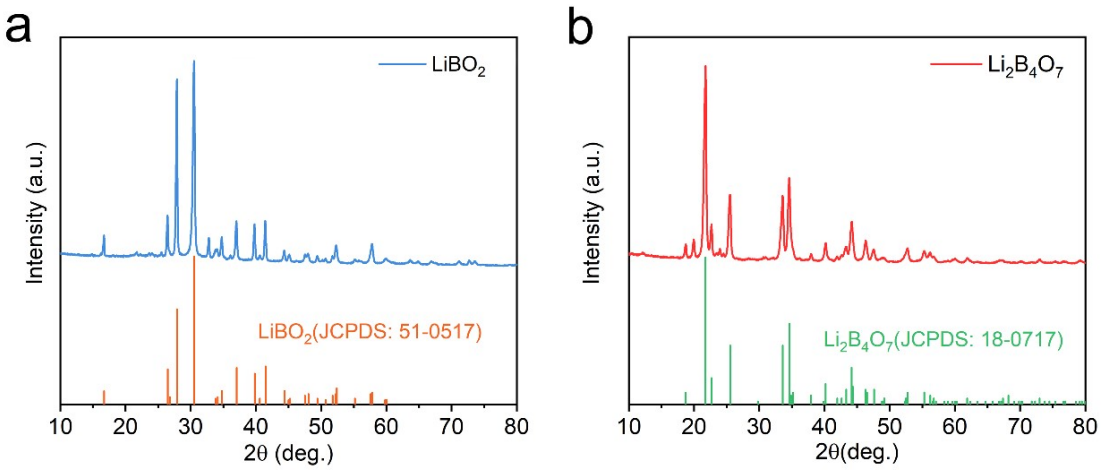

Fig. S1. XRD pattern of the (a) $LiBO_2$, which is correspond with the standard PDF card #51-0517, and (b) $Li_2B_4O_7$, which matches the standard PDF card #18-0717.

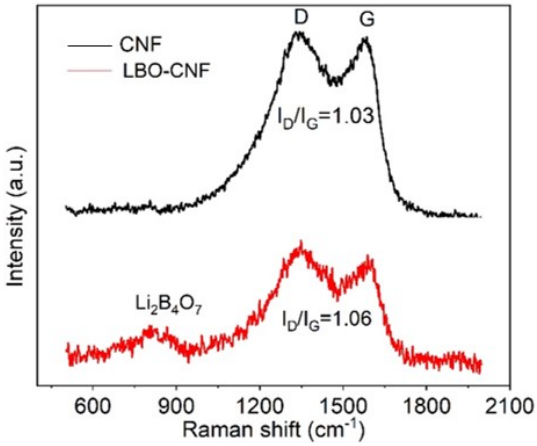

Fig. S2. Raman spectra of the CNF and LBO-CNF. The ratio of I_D/I_G indicates the defects structure of CNF skeleton.

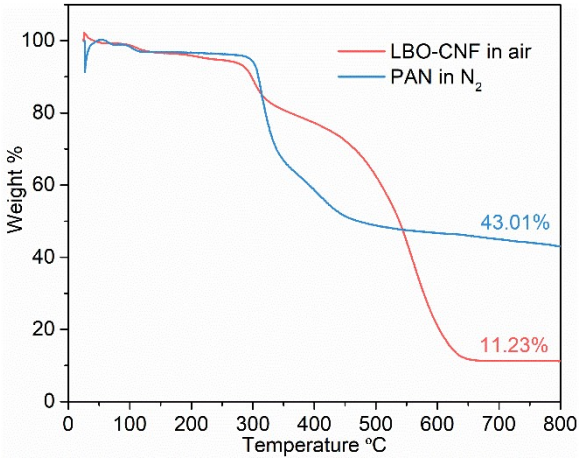

Fig. S3. TGA curves of LBO-CNF in air and CNF under nitrogen atmosphere.

The LBO-CNF was derived from LBO-PAN fiber. When the themogravimetric analysis of LBO-PAN were carried out in air, obviously only LBO left and PAN became CO_2. Hence the 11.23% indicates the content of LBO in pristine LBO-PAN. When the themogravimetric analysis of PAN fiber were carried out under nitrogen atmosphere, the PAN fiber will transform into CNF, here 43.01% represents the conversion ratio of the PAN fiber to CNF. Therefore, the content of LBO in LBO-CNF could be calculated as follows:

$$\frac{m_{LBO}}{m_{LBO-CNF}}$$

$$m_{LBO} = 11.23\%\, m_{LBO-PAN}$$

$$m_{LBO-CNF} = m_{LBO} + m_{CNF}$$

$$m_{CNF} = 43.01\%\, m_{PAN}$$

$$m_{PAN} = (1 - 11.23\%) m_{LBO-PAN}$$

Thus,

$$\frac{m_{LBO}}{m_{LBO-CNF}} = \frac{11.23\%\, m_{LBO-PAN}}{11.23\%\, m_{LBO-PAN} + 43.01\%\, (1 - 11.23\%) m_{LBO-PAN}} = 22.7\%$$

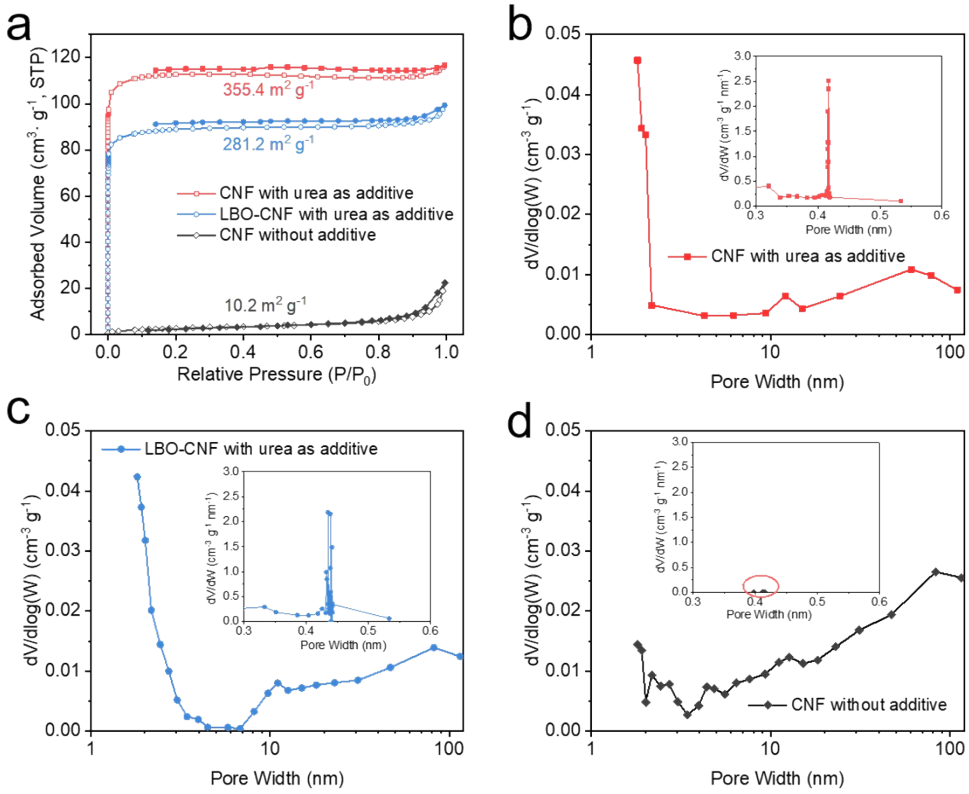

Fig. S4. N_2 isothermal adsorption-desorption curves of CNF derived from PAN. BJH pore-size distribution of

(b) CNF with urea, (c) LBO-CNF with urea, and (d) CNF without urea. The inset shows the HK pore-size distribution.

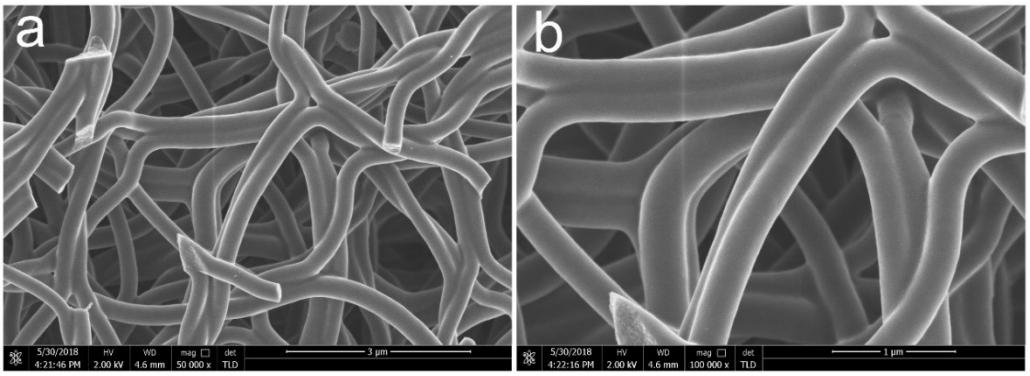

Fig. S5. SEM image of the fracture of the CNF. The surface of the CNF is smooth.

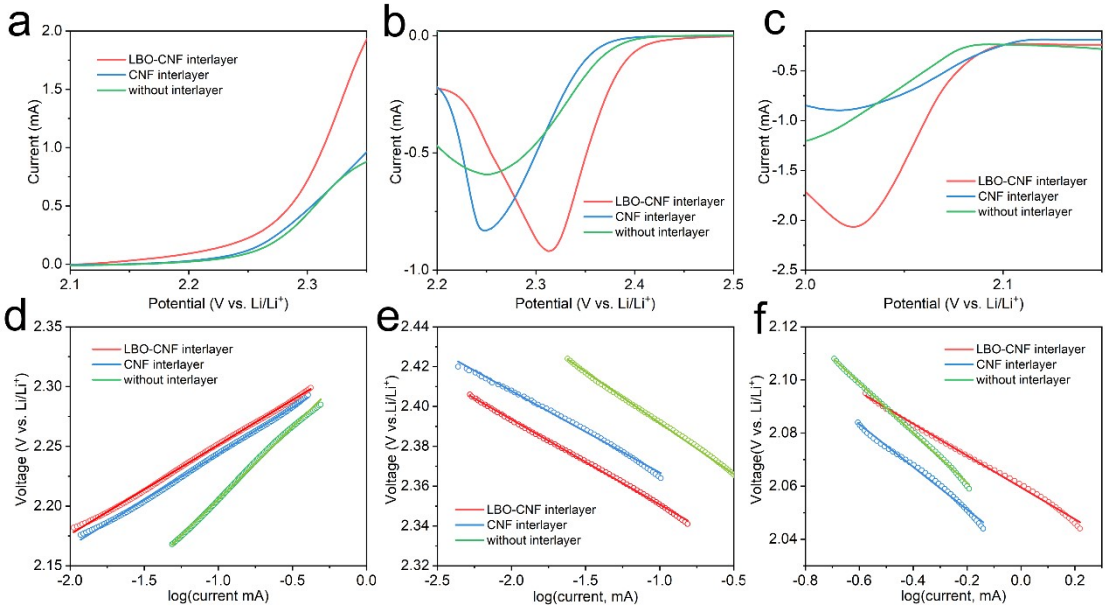

Fig. S6. (a-c) The enlarged anodic and cathodic sections of the CV curves. (d-f) Tafel plots derived from the potentiostatic polarization curves. The corresponding values are listed in Table S4.

T**able S1**. Tafel plots derived from the potentiostatic polarization curves of the battery with LBO-CNF, CNF interlayer and without interlayer.

sample	Tafel slop (mV dec^{-1})		
	anodic	cathodic-i	cathodic-ii
LBO-CNF	0.074E-4	0.041E-4	0.059E-4
CNF	0.077E-4	0.043E-4	0.080E-4
Without interlayer	0.121E-4	0.051E-4	0.094E-4

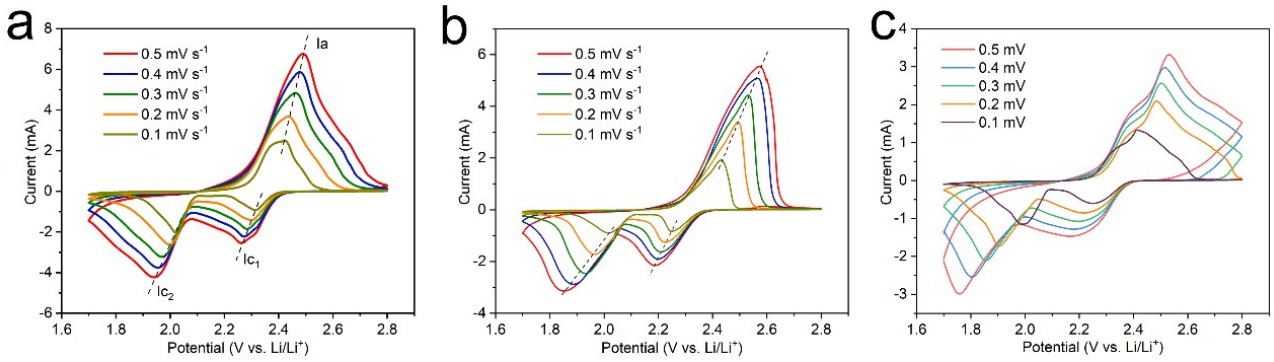

Fig. S7. CV curves of (a) LBO-CNF interlayer, (b) CNF interlayer, and (c) without interlayer at different scan rates from 0.1 to 0.5 mV s^{-1}.

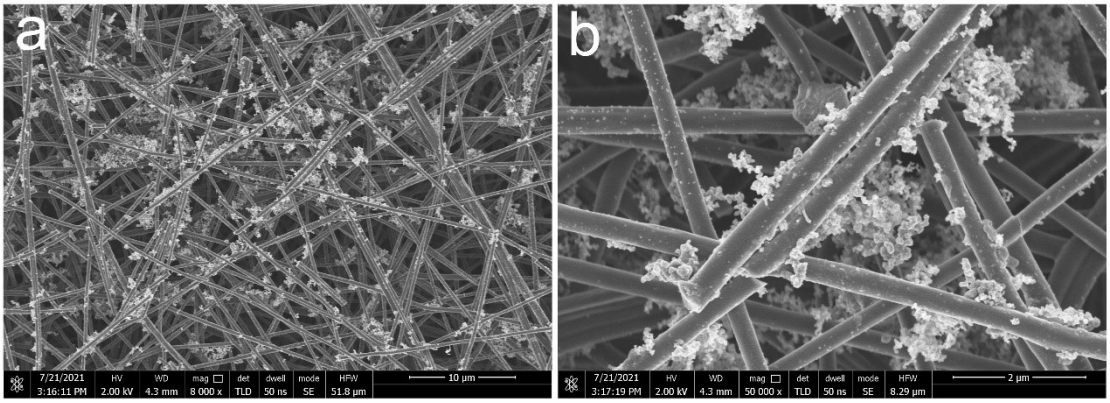

Fig. S8. SEM images of the CNF sprayed Acetylene Black nanoparticles.

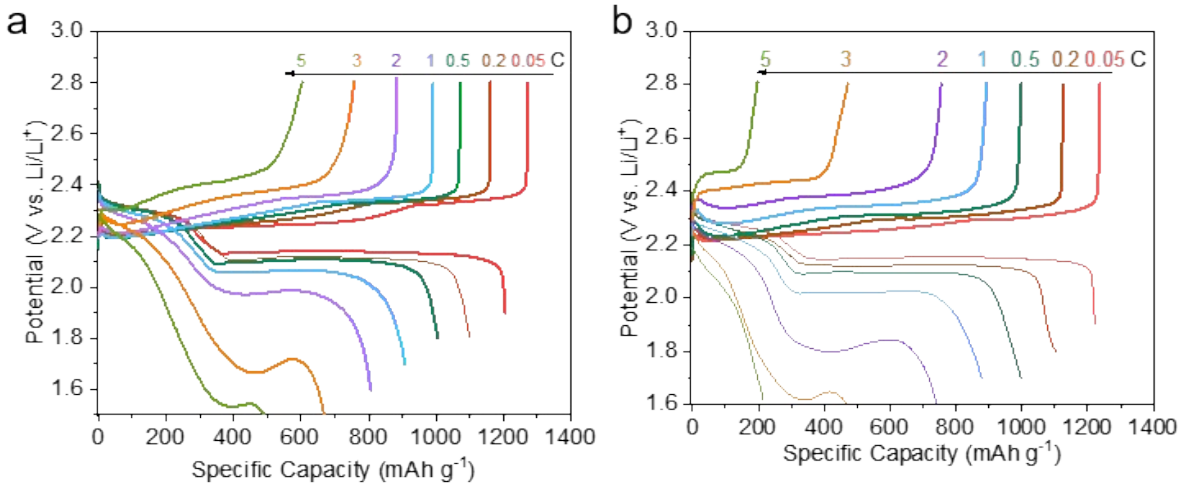

Fig. S9. Discharge and charge profiles of Li-S battery at different current rates with (a) CNF interlayer and (b) without interlayer.

Table S2. The fitting results of the equivalent circle of the fresh batteries with LBO-CNF, CNF interlayer and without interlayer.

sample	Impedance (ohm)	
	R_e	R_{ct}
LBO-CNF	2.9	90.8
CNF	1.3	109.2
Without interlayer	4.8	122.8

Table S3. The fitting results of the equivalent circle of the cycled cells with LBO-CNF, CNF interlayer and without interlayer.

sample	Impedance (ohm)		
	R_e	R_{ct}	R_{SEI}
LBO-CNF	2.3	9.8	7.1
CNF	3.2	20.6	8.5
Without interlayer	3.1	38.6	11.6

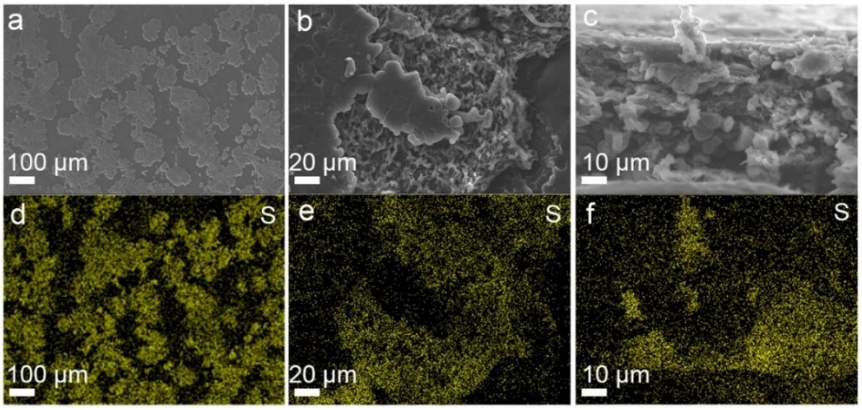

Fig. S10. SEM images and relative EDX mapping of lithium of the disassembled Li-S batteries without interlayer. (a-c) top view, (d-f) top view enlarged, and (g-i) side view.

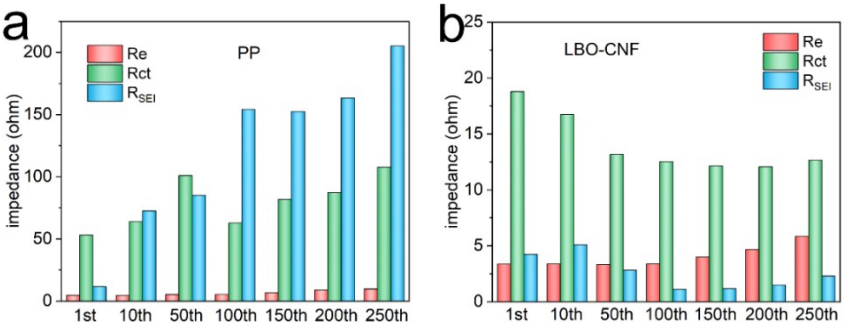

Fig. S11. EIS fitting values of Li-S battery (a) without interlayer and (b) with LBO-CNF interlayer at different cycle.

Table S4. The fitting results of the equivalent circle of the battery without interlayer at different cycles at 0.2 C.

cycle	Impedance (ohm)		
	R_e	R_{ct}	R_{SEI}
1st	4.7	53.2	11.6
10th	4.6	63.7	72.6
50th	5.3	100.9	85.2
100th	5.4	62.8	154.3
150th	6.7	81.9	152.5
200th	8.9	87.4	163.4
250th	9.8	107.8	205.2

Table S5. The fitting results of the equivalent circle of the battery with LBO-CNF interlayer at different cycles at 0.2 C.

cycle	Impedance (ohm)		
	R_e	R_{ct}	R_{SEI}
1st	3.3	18.8	4.3
10th	3.4	16.7	5.1
50th	3.3	13.2	2.8
100th	3.4	12.5	1.1
150th	4.1	12.2	1.2
200th	4.7	12.1	1.5
250th	5.8	12.6	2.3

Table S6. The content of sulfur in the cathode and with interlayer included.

Sulfur loading (mg cm^{-2})	Interlayer (mg cm^{-2})	Sulfur content in the cathode	Sulfur content with interlayer included
~ 1.8	~ 0.54	65%	54.4%
~ 2.5	~ 0.54	65%	57.0%
~ 3.5	~ 0.54	65%	59.1%